International Journal of Information & Communication Technology



Volume 2- Number 1- May 2010 (pp.11-19)

A Maximum Likelihood Frequency Offset Estimation with Improved Range and Performance in OFDM Systems

H. Nezamfar

Electrical Engineering Department
Iran University of Science and Technology
Tehran, Iran
nezamfar@ece.neu.edu

M. H. Kahaei

Electrical Engineering Department
Iran University of Science and Technology
Tehran, Iran
kahaei@iust.ac.ir

Received: December 23, 2008- Accepted: December 17, 2009

Abstract—Maximum Likelihood (ML) estimation of the frequency offset between the transmitter and the receiver from known transmitted preambles is the dominant technique for the estimation of Carrier Frequency Offset (CFO) in OFDM systems. A general formulation of ML detection problem for OFDM systems is provided in this paper and it is described how different ML techniques can be treated as special cases. In addition, major newly proposed ML techniques are compared in a unified simulation framework in the presence of AWGN and their performance in terms of estimation range and complexity is compared. Furthermore, we proposed two new preamble structures which have comparable complexity to the simplest available methods while their estimation ranges are fairly large, comparable to the largest achieved ranges.

Keywords-Orthogonal frequency division multiplexing (OFDM), Carrier Frequency, Offset, Maximum Likelihood.

I. INTRODUCTION

Orthogonal Frequency Division Multiplexing (OFDM) is the modulation used for many high speed communication systems. OFDM has the main advantages of being bandwidth efficient and robust against multi-path fading, which make it suitable for wireless systems in crowded environments. OFDM has been used in several standards including IEEE802.11, Hiperlan2 [1], IEEE802.16 [2] and DVB-T [3]. However, the main challenge in using OFDM is that the system performance heavily depends on the synchronization between the transmitter and the receiver [4 - 6]. For example, the system performance can substantially degrade due to

a small offset in the carrier frequency between the transmitter and the receiver. The doppler effect caused by the mobility of the transmitter or receiver can also introduce a virtual offset.

The CFO reduces the system performance since it degrades the orthogonality among the OFDM sub-carriers. Substantial amount of work has been done in order to overcome the CFO problem by estimating and compensating the offset. Most of the proposed methods are based on joint maximum likelihood detection of the channel response and the frequency offset from known preamble sequences [7 - 11]. Preambles are sequences of known data sent at the beginning of a burst of data, especially designed to ease the estimation procedure. Such methods estimate

The first major ML-based CFO estimation technique was proposed by Schmidl and Cox [8]. In this method, two identical preamble sequences are transmitted, and the CFO is estimated at the receiver by a simple correlation. However, the range of estimation technique is limited by the OFDM symbol rate since the correlation output is periodic with respect to the frequency offset. A more sophisticated technique was proposed by Morelli and Mengali [10], in which a cascade of several shorter identical preambles are transmitted and the frequency offset is estimated by pair-wise correlation of all the preambles and combining the results. The resulting estimator is still periodic with respect to the frequency offset; however, the period is larger than the former method, leading to larger estimation range at the cost of larger complexity. To eliminate the periodicity, Minn and Tarasak [11] proposed another preamble structure in which redundant symbols are inserted between the preamble symbols of the former method, leading to a less regular preamble structure. This irregularity is desirable as it leads to a larger estimation range. Nonetheless, both methods using multiple preamble symbols require a sophisticated detection hardware incorporating an FFT block with a reasonably large block size.

In this paper, we formulate the ML CFO estimation technique for an arbitrary preamble sequence and propose two new preamble structures that eliminate the periodicity in the estimation function and require a simple detection hardware. We further compare the performance and complexity of previously proposed techniques with the proposed techniques through MATLAB simulations.

The rest of this paper is organized as follows. In Section II, the signal model and the general Maximum likelihood formulation are explained. In Section III, we explain how different estimation techniques can be described as special cases. In Section IV, the new preamble structures are presented. In Section V, we compare the performance of the three methods explained in Section III with our proposed methods in a unified simulation environment and Section VI concludes the paper.

II. SIGNAL MODEL AND ML FORMULATION

In OFDM systems, a block of data is transmitted as an OFDM symbol. A block diagram of such a system is shown in Fig. 1. Assuming a symbol size equal to N (where N is a power of 2), the transmitted block of data at time i ($i \ge 0$) is denoted by

$$\mathbf{s}_i \stackrel{\Delta}{=} \begin{bmatrix} s_i(0) & s_i(1) & \dots & s_i(N-1) \end{bmatrix}^{\mathrm{T}}$$
 (1)

where $[.]^T$ shows transposition. Each block is passed through the IDFT as

$$\bar{\mathbf{s}}_i = \mathbf{F}^H \mathbf{s}_i \tag{2}$$

where $\mathbf{F}^{\mathbf{H}}$ is the hermitian transposition of the the unitary discrete Fourier transform (DFT) matrix, \mathbf{F} , of size N defined by

$$[\mathbf{F}]_{ik} \stackrel{\triangle}{=} \frac{1}{\sqrt{N}} e^{\frac{-j2\pi ik}{N}}, \quad j = \sqrt{-1}$$

$$i, k = \{0, 1, \dots, N-1\}$$
(3)

A cyclic prefix of length P is added to each transformed block of data and then transmitted through the channel. An FIR model with L+1 taps is assumed for the channel, *i.e.*,

$$\mathbf{h} = \begin{bmatrix} h_0 & h_1 & \dots & h_L \end{bmatrix}^{\mathbf{T}} \tag{4}$$

with $L \leq P$ in order to completely avoid the ISI. At the receiver, the received samples corresponding to the transmitted block $\bar{\mathbf{s}}_i$ are collected into a vector, after discarding the received cyclic prefix samples. The received block of data after being distorted by the frequency offset can be written as:

$$\bar{\mathbf{y}}_i = \Phi_i(z)\mathbf{H}^c\bar{\mathbf{s}}_i + \bar{\mathbf{v}}_i \tag{5}$$

where

$$\mathbf{H}^{c} = \begin{bmatrix} h_{0} & h_{1} & \cdots & h_{L} & 0 & \cdots & 0 \\ 0 & h_{0} & h_{1} & \cdots & h_{L} & \ddots & 0 \\ \vdots & \ddots & \ddots & \ddots & \ddots & \ddots & \ddots \\ 0 & \cdots & 0 & h_{0} & h_{1} & \cdots & h_{L} \\ \vdots & \ddots & \ddots & \ddots & \ddots & \ddots & \ddots \\ h_{2} & \cdots & h_{L} & 0 & \cdots & h_{0} & h_{1} \\ h_{1} & \cdots & h_{L} & 0 & \cdots & 0 & h_{0} \end{bmatrix}$$

$$(6)$$

is an $N \times N$ circulant matrix and $\bar{\mathbf{v}}_i$ is additive white noise at the receiver. The $N \times N$ matrix $\Phi_i(z)$ models the effect of frequency offset defined as

$$\Phi_{i}(z) = z^{i(N+p)} \begin{bmatrix} 1 & 0 & \cdots & 0 \\ 0 & z & \ddots & \vdots \\ \vdots & \ddots & \ddots & 0 \\ 0 & \cdots & 0 & z^{N-1} \end{bmatrix}$$
(7)

where z is the phase rotation due to frequency offset from one element in \bar{y}_i to the next given as:

$$z = e^{j\theta} = e^{j2\pi \frac{\Delta f}{f_s}} \tag{8}$$

where f_s and Δf are the sampling frequency and the frequency offset, respectively. Which is assumed constant.[12-15] The objective is to estimate Δf , or equivalently, z. It is known that \mathbf{H}^c can be diagonalized by the DFT matrix as $\mathbf{H}^c = \mathbf{F}^H \Lambda \mathbf{F}$ [16], where

$$\Lambda = \operatorname{diag}\{\lambda\} \tag{9}$$

and the vector λ is related to \mathbf{h} via

$$\lambda = \sqrt{\mathbf{N}} \mathbf{F}^{\mathbf{H}} \begin{bmatrix} \mathbf{h} \\ \mathbf{0}_{(N-(L+1))\times 1} \end{bmatrix}$$
 (10)

¹We would use the notation diag{.} in both directions, *i.e.*, $\Lambda = \text{diag}\{\lambda\}$ and $\lambda = \text{diag}\{\Lambda\}$.

Fig. 1. A block diagram of an OFDM system with frequency offset.

Substituting for \mathbf{H}^c in (5),

$$\bar{\mathbf{y}}_i = \Phi_i(z) \mathbf{F}^H \mathbf{\Lambda} \mathbf{s}_i + \bar{\mathbf{v}}_i \tag{11}$$

Now assume that M received $\bar{\mathbf{y}}_i$ vectors, i = $\{0,\ldots,M-1\}$, are collected at the receiver. The maximum likelihood estimates of $\{\lambda, z\}$ can be found by solving[17]

$$\{\hat{\lambda}, \hat{z}\} = \arg\min_{\lambda, z} [J_{ML}(\lambda, z)]$$
 (12)

where

$$J_{ML}(\lambda, z) = \sum_{i=0}^{M-1} \|\bar{\mathbf{y}}_i - \Phi_i(z)\mathbf{F}^H \mathbf{\Lambda} \mathbf{s}_i\|^2$$
 (13)

where ||.|| denotes the Euclidean norm of the vector. Let us denote diag $\{s_i\}$ with S_i . Then, $\Lambda s_i = S_i \lambda$. Grouping the terms in (13) into a vector results in

$$J_{ML}(\lambda, z) = \begin{bmatrix} \bar{\mathbf{y}}_0 \\ \vdots \\ \bar{\mathbf{y}}_{M-1} \end{bmatrix} - \underbrace{\begin{bmatrix} \Phi_0(z) \mathbf{F}^H \mathbf{S}_0 \\ \vdots \\ \Phi_{M-1}(z) \mathbf{F}^H \mathbf{S}_{M-1} \end{bmatrix}}_{\mathbf{X}} \lambda \|^2 \quad (14)$$

which is a least-squares problem whose solution is given by $\hat{\lambda} = (\mathbf{X}^{\mathbf{H}}\mathbf{X})^{-1}\mathbf{X}^{\mathbf{H}}\mathbf{Y}$, or,

$$\hat{\lambda}(z) = \left(\sum_{i=0}^{M-1} \mathbf{S}_i^H \mathbf{S}_i\right)^{-1} \left(\sum_{i=0}^{M-1} \mathbf{S}_i^H \mathbf{F} \Phi_i^H(z) \bar{\mathbf{y}}_i\right)$$
(15)

where we used the fact that $\Phi_i^H(z)\Phi_i(z)$ and $\mathbf{F}^H\mathbf{F}$ are identity matrices. Note that λ is a function of z and J_{ML} needs to be minimized over z as well. Substituting the least-squares solution, the resulting minimum cost function is given by

$$J_{ML}(\hat{\lambda}, z) = \|\mathbf{Y}\|^2 - \|\mathbf{X}\hat{\lambda}\|^2$$
 (16)

Let us define the diagonal Hermitian matrix \mathbf{D} as

$$\mathbf{D} = \sum_{i=0}^{M-1} \mathbf{S}_i^H \mathbf{S}_i \tag{17}$$

Calculating the term $\|\mathbf{X}\hat{\lambda}\|^2$ through $\hat{\lambda}^H\mathbf{X}^H\mathbf{X}\hat{\lambda}$ and

substituting $\mathbf{X}^H \mathbf{X} = \mathbf{D}$ leads to²

$$\|\mathbf{X}\hat{\lambda}\|^{2} = \left(\sum_{i=0}^{M-1} \mathbf{S}_{i}^{H} \mathbf{F} \boldsymbol{\Phi}_{i}^{H}(z) \bar{\mathbf{y}}_{i}\right)^{H}.$$

$$\mathbf{D}^{-1} \left(\sum_{i=0}^{M-1} \mathbf{S}_{i}^{H} \mathbf{F} \boldsymbol{\Phi}_{i}^{H}(z) \bar{\mathbf{y}}_{i}\right)$$

$$= \sum_{i=0}^{M-1} \sum_{l=0}^{M-1} \bar{\mathbf{y}}_{i}^{*} \boldsymbol{\Phi}_{i}(z) \mathbf{F}^{H} \mathbf{S}_{i} \mathbf{D}^{-1} \mathbf{S}_{l}^{H} \mathbf{F} \boldsymbol{\Phi}_{l}^{H}(z) \bar{\mathbf{y}}_{l}$$
(18)

Noting that the first term in (16) is independent of z, the problem of minimizing (16) with respect to zbecomes

$$\hat{z} = \arg\max_{z} [I_{ML}(z)] \tag{19}$$

where $I_{ML}(z) = \|\mathbf{X}\hat{\lambda}\|^2$, or,

$$I_{ML}(z) = \sum_{i=0}^{M-1} \bar{\mathbf{y}}_i^* \Phi_i(z) \mathbf{C}_{ii} \Phi_i^H(z) \bar{\mathbf{y}}_i + 2\operatorname{Re} \left(\sum_{i=0}^{M-1} \sum_{l=0, l < i}^{M-1} \bar{\mathbf{y}}_i^* \Phi_i(z) \mathbf{C}_{il} \Phi_l^H(z) \bar{\mathbf{y}}_l \right)$$
(20)

where $\mathbf{C}_{il} = \mathbf{F}^H \mathbf{S}_i \mathbf{D}^{-1} \mathbf{S}_l^H \mathbf{F}$. Since $\mathbf{S}_i \mathbf{D}^{-1} \mathbf{S}_l^H$ is a diagonal matrix, C_{il} is a circulant matrix whose first row is defined as:

$$\mathbf{c_{il}^{T}} = \sqrt{N} \mathbf{F}^{H} \operatorname{diag}(\mathbf{S}_{i} \mathbf{D}^{-1} \mathbf{S}_{l}^{H})$$
 (21)

The above equation then results in (22) (shown at the top of the following page). Substituting (22) in

²Assume that D is full-rank by design. If certain samples in the training symbol need to be zero (e.g.to control the peak-to-average power ratio), corresponding rows in (11) can be removed, which makes D full rank again.

(20) results in a summation of polynomials as

$$I_{ML}(z) = \sum_{i=0}^{M-1} I_{ii}(z) + 2\operatorname{Re}\left(\sum_{i=0}^{M-1} \sum_{l=0, l < i}^{M-1} I_{il}(z)\right)$$
(23)

where $I_{il}(z)$ is determined by

$$z^{(i-l)(N+P)} \left(\sum_{m=-N+1}^{N-1} \mathbf{c}_{il}(\text{mod}(m,N)) R_{il}(m) z^{-m} \right)$$
(24)

where $R_{il}(m)$, $m = \{-N+1, ..., N-1\}$, is the cross correlation between \bar{y}_i and \bar{y}_l defined as

$$R_{il}(m) = \sum_{j=\max(0,m)}^{\min(N-1,N-1+m)} \bar{\mathbf{y}}_{i}^{*}(j-m)\bar{\mathbf{y}}_{l}(j) \quad (25)$$

All of today's standardized OFDM-based systems use training symbols from a QPSK constellation. In such cases, the term $I_{ii}(z)$ is a constant and does not depend on z. Therefore, it can be ignored and the problem of frequency offset estimation reduces to maximizing the following polynomial:

$$I'_{ML}(z) = \text{Re}\left(\sum_{i=0}^{M-1} \sum_{l=0, l < i}^{M-1} I_{il}(z)\right)$$
 (26)

In general, $I_{il}(z)$ is a polynomial with 2N-1 terms.

III. SPECIAL CASES

The problem formulation in the previous section is sufficiently general to include any ML CFO estimation method with QPSK preambles. In this section, we describe how the three previously proposed methods can be explained within this framework.

A. Schmidl and Cox's estimatoin method

This method originally was the first major maximum likelihood estimation scheme developed [8] to overcome the problem of carrier frequency offset. This method suggests the use of two identical preambles as shown in Fig. 2(a). This choice of preamble corresponds to $\overline{s}_1 = \overline{s}_0$ in the formulation of Section II. In this case, c_{10} becomes

The cost function (26) then reduces to

$$I'_{ML}(z) = \operatorname{Re}\left(z^{N}\mathbf{c}_{10}(0)R_{10}(0)\right)$$
 (27)

where according to (25), $R_{10}(0)$ is now given by

$$R_{10}(0) = \sum_{j=0}^{N-1} \bar{\mathbf{y}}_1^*(j) \bar{\mathbf{y}}_0(j) = \bar{\mathbf{y}}_1^* \bar{\mathbf{y}}_0$$

The solution to maximizing (27) is given by

$$\hat{z}^N = e^{-j\angle \bar{\mathbf{y}}_1^* \bar{\mathbf{y}}_0} \tag{28}$$

where it is related to the frequency offset through

$$\hat{z}^N = e^{j2\pi(N)\frac{\Delta f}{f_s}} \tag{29}$$

The above equation results in a unique estimation for Δf only if $|\Delta f| < \frac{1}{2} \frac{f_s}{(N)}$. In other words, estimation range is equal to the OFDM sub-carrier spacing.

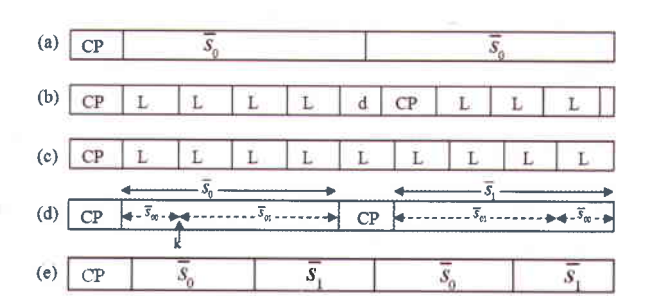


Fig. 2. Several preamble structures with fixed length, (a)The preamble structure of Schmidl [8]. (b)The preamble structure of Minn [11]. (c)The preamble structure of Morelli [10]. (d)The first proposed preamble structure. [18] (e)The second proposed preamble structure.

B. Minn and Tarasak's estimation method

Fig. 2(b) shows the optimum preamble structure proposed in [11]. In this method, the preamble consists of multiple identical symbols of length P, where P is the length of cyclic prefix equal to L the length of channel dispersion. The set of all preamble symbols is divided to two (or more) subsets and a space of d samples is inserted between the two subsets. The first symbol of length P at the beginning of the preamble, and the symbol immediately after the d redundant samples serve as cyclic prefix and are discarded.



 $\mathbf{c}_{10} = \left[\begin{array}{cccc} 1 & 0 & \dots & 0 \end{array} \right]$

$$d = \left(k_0 + \frac{n_1}{n_2}\right)P\tag{30}$$

where k_0, n_1, n_2 are nonnegative integers with $n_1 = 0$ if $n_2 = 1, n_1 \in \{1, ..., n_2 - 1\}$ if $n_2 > 1$, and P/n_2 is an integer. Then it can be shown that the cost function (26) reduces to

$$I_{ML}^{'}(z) = \text{Re}\left(\sum_{0}^{N_{\beta}-1} \beta_{n} z^{\frac{nP}{n_{2}}}\right)$$
 (31)

where β_n is the summation of all the correlation terms I_{il} which have the same phase factor $(\theta_l - \theta_i) =$ $n(2\pi \frac{\Delta f}{f}P/n_2)$.

$$\beta_n = \sum_{\{i,l\}:\theta_l - \theta_i = n(2\pi \frac{\Delta f}{f_s} P/n_2)} I_{il}$$
 (32)

If $k_0 = n_1 = 0$, then $N_\beta = U - 1$, U is the number of preamble symbols of length P(U = 7 in Fig. 2(b)). If $n_1 = 0$ and $k_0 > 0$, then $N_{\beta} = U - 1 + k_0$. If $n_1 > 0$, then $N_{\beta}=n_2(U+k_0)+n_1$. Then the frequency offset estimate is given by

$$\frac{\Delta f}{f_s} = \frac{n_2}{PN_{fft}} \arg \max_{-N_{fft}/2 \le m < N_{fft}/2} \{ \operatorname{Re}[F_{N_{fft}}\beta] \}$$
(33)

where $F_{N_{fft}}\beta$ gives the N_{fft} point FFT of β [11].

Equation (31) is similar to equation (27) except that it contains several additional terms. The parameter d can be set such that it maximizes the period of the cost function (31), and increase the estimation range. However, as shown in equation (33), obtaining the frequency offset requires an FFT operation on the vector β . Choosing a small FFT size (N_{fft}) will lead to quantization errors in the estimation while increasing N_{fft} leads to more complexity. In addition, the introduction of a gap of d samples in the preamble sequence introduces redundancy, which can affect the performance of the estimation technique in noisy environments.

C. Morelli and Mengali's estimation method

This method was introduced prior to the method described in the previous section and can be considered as a special case of Minn's method, where d = 0. The preamble structure is shown in Fig. 2(c). Due to the absence of the redundant samples in the preamble, only one cyclic prefix is required. The cost function, therefore reduces to

$$I'_{ML}(z) = \operatorname{Re}\left(\sum_{0}^{U-1} \beta_n z^{nP}\right)$$
 (34)

Compared to (27), this method can increase the period of the cost function by a factor of N/P. However, it still requires an FFT operation to estimated the frequency offset and its performance can be limited by FFT block size.

IV. THE PROPOSED PREAMBLE SEQUENCE AND ESTIMATION TECHNIQUE

In this section we propose two new preamble structures that eliminated the periodicity in the ML cost function, and therefore, increase the estimation range, but require simple estimation hardware. Fig. 2(d) shows the first proposed preamble sequence. The preamble consists of two symbols where the second symbol is a cyclically shifted (rotated) version of the first one as shown in Fig. 2(d).

Let

$$\mathbf{s}_1 = \sqrt{N} \operatorname{diag}\{[\mathbf{F}^{\mathbf{H}}]_k\} \mathbf{s}_0 \tag{35}$$

where $[\mathbf{F}^{\mathbf{H}}]_k$ is the k_{th} row of the IDFT matrix $\mathbf{F}^{\mathbf{H}}$ and F is the DFT matrix in (3), $k = \{1, ..., N-1\}$. (this is equivalent to \bar{s}_1 being a cyclically shifted version of \bar{s}_0 by k samples). Fig. ?? shows a demonstration of transmitting the preamble.

Note that k = 0 reduces to $s_1 = s_0$. In this case, the vector \mathbf{c}_{10} in (21) becomes

where the only non-zero term is located at the $(k+1)_{th}$ position. The cost function (26) then reduces to

$$\begin{split} I'_{ML}(z) &= I_{10}(z) \\ &= \operatorname{Re} \left(z^{N+P} \left(R_{10}(-N+k) z^{N-k} + R(k)_{10} z^{-k} \right) \right) \\ &= \operatorname{Re} \left(R_{10}(-N+k) z^{2N+P-k} + R_{10}(k) z^{N+P-k} \right) \end{aligned} \tag{36}$$

where we used the fact that $c_{10}(k) = 1$. Note that only terms corresponding to m = k and m = N + kremain and k can be chosen such that the cost function is not periodic with respect to theta.

The cross correlation terms $R_{10}(-N+k)$ and $R_{10}(k)$ are defined by (25) as

$$R_{10}(k) = \sum_{j=k}^{N-1} \bar{\mathbf{y}}_1^*(j-k)\bar{\mathbf{y}}_0(j)$$
 (37)

$$R_{10}(-N+k) = \sum_{j=0}^{k-1} \bar{\mathbf{y}}_1^* (N-k+j) \bar{\mathbf{y}}_0(j)$$
 (38)

The above expressions can be rewritten in vector product format as

$$a_{1} \stackrel{\triangle}{=} R_{10}(k)$$

$$= \begin{bmatrix} \bar{\mathbf{y}}_{1}(0) \\ \vdots \\ \bar{\mathbf{y}}_{1}(N-k-1) \end{bmatrix}^{H} \begin{bmatrix} \bar{\mathbf{y}}_{0}(k) \\ \vdots \\ \bar{\mathbf{y}}_{0}(N-1) \end{bmatrix}$$
(39)

and

$$a_{2} \stackrel{\triangle}{=} R_{10}(-N+k)$$

$$= \begin{bmatrix} \bar{\mathbf{y}}_{1}(N-k) \\ \vdots \\ \bar{\mathbf{y}}_{1}(N-1) \end{bmatrix}^{H} \begin{bmatrix} \bar{\mathbf{y}}_{0}(0) \\ \vdots \\ \bar{\mathbf{y}}_{0}(k-1) \end{bmatrix}$$

$$(40)$$

Now the objective is to minimize $I'_{ML}(z)$ with respect to Δf (or equivalently with respect to θ in (8)).

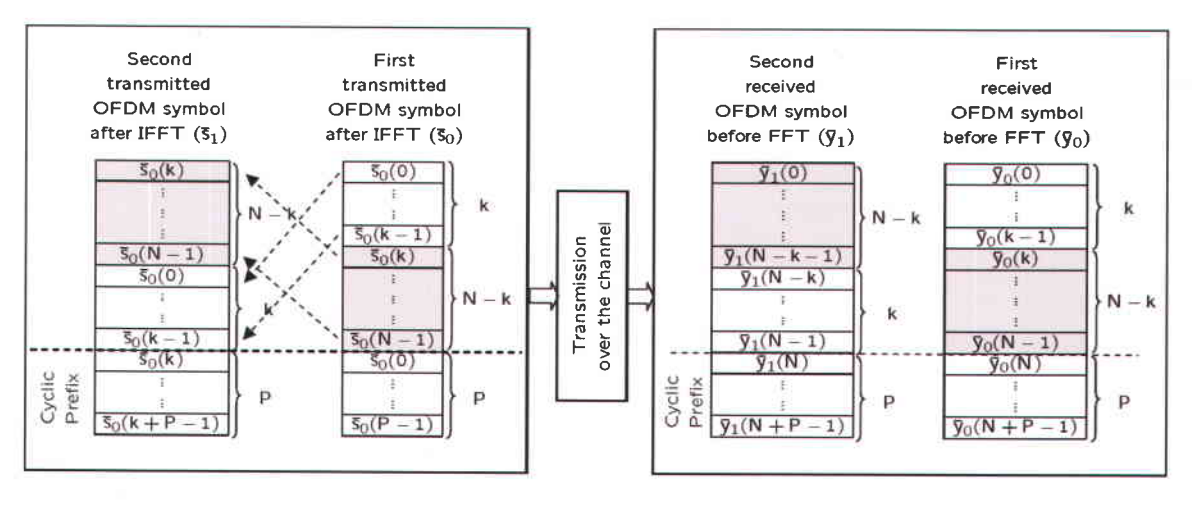


Fig. 3. A demonstration of two transmitted OFDM symbols corresponding to the structure in (35).

Differentiating $I_{ML}^{'}(z)$ with respect to θ and solving for $\frac{dI_{ML}^{'}(z)}{d\theta}=0$ leads to

$$(2N + P - k)|a_2| \sin [(2N + P - k)\theta + \angle a_2] + (N + P - k)|a_1| \sin [(N + P - k)\theta + \angle a_1] = 0$$
(41)

It can be easily shown that both the \sin arguments are close to zero (see Appendix), therefore applying $\sin \alpha \approx \alpha$ results in

$$\hat{\theta} = -\frac{(2N+P-k)|a_2| \angle a_2 + (N+P-k)|a_1| \angle a_1}{(2N+P-k)^2 |a_2| + (N+P-k)^2 |a_1|}$$
(42)

and the estimate for frequency offset is given by

$$\Delta \hat{f} = \frac{f_s \hat{\theta}}{2\pi} \tag{43}$$

Equations (42) and (43) indicate that a simple detection hardware is necessary for detecting the CFO while the periodicity present in cost functions (27) and (34) is eliminated.

The above cost function for large frequency offsets leads to an ambiguity in the phase of the two correlation terms a_1 and a_2 . In order to avoid this ambiguity we define two new parameters m_1 and m_2 . We can show the phase of the parameter a_1 generally as $m_1\pi + \angle a_1$. Where $\angle a_1$ is between $-\pi$ and π and m_1 is an integer, the phase rotation coefficient. In a similar way we can show the phase of a_2 as $m_2\pi + \angle a_2$. Substituting these new phase definitions in the cost function (42) the new cost function is:

$$\hat{\theta} = -\frac{(2N+P-k)|a_2|(m_2\pi+\angle a_2)}{(2N+P-k)^2|a_2|+(N+P-k)^2|a_1|} - \frac{(N+P-k)|a_1|(m_1\pi+\angle a_1)}{(2N+P-k)^2|a_2|+(N+P-k)^2|a_1|}$$
(44)

Here again we used the $sin\alpha=\alpha$ for both a_1 and a_2 . Between all $\hat{\theta}(m_1,m_2)$ values the one that maximizes the cost function (36) is the optimum estimate. The terms m_1 and m_2 are unknowns. Considering Δf_{max} as the maximum desired frequency offset we

can define the following boundaries for m_1 and m_2 :

$$-\frac{ang(a_1)}{\pi} - \frac{2(N+P-k)\Delta f_{max}}{f_s} \le m_1$$

$$m_1 \le \frac{2(N+P-k)\Delta f_{max}}{f_s} - \frac{ang(a_1)}{\pi}$$
(45)

$$-\frac{ang(a_2)}{\pi} - \frac{2(2N+P-k)\Delta f_{max}}{f_s} \le m_2$$

$$m_2 \le \frac{2(2N+P-k)\Delta f_{max}}{f_s} - \frac{ang(a_2)}{\pi}$$
(46)

The above boundaries are achieved by considering m_1 and m_2 as independent variables. Taking a deeper look at (39) and (40) shows that m_1 and m_2 are not independent variables. They have the following relation:

$$m_2 = -\left[m_1 + N\frac{\theta}{\pi} + \frac{\angle a_2 - \angle a_1}{\pi}\right]$$
 (47)

Considering the above relation we can make the boundaries even narrower than before. Considering m_1 and m_2-m_1 as independent variables the boundaries of m_1 are same as before but the new boundaries for m_2 are:

$$m_{1} - \frac{ang(a_{2}) - ang(a_{1})}{\pi} - N \frac{2\Delta f_{\text{max}}}{f_{s}} \leq m_{2}$$

$$m_{2} \leq N \frac{2\Delta f_{\text{max}}}{f_{s}} + m_{1} - \frac{ang(a_{2}) - ang(a_{1})}{\pi}$$
(48)

Using the m_1 and m_2 terms we only examine a few pairs of m_1 and m_2 to find the correct estimate of the carrier frequency offset, for example only 60 pairs must be compared for a frequency offset equal to 2 sub-carrier spacing. In this method the boundaries of m_2 are dynamically assigned by the boundaries of m_1 . As there are side lobes in the cost function, in presence of noise it is possible to have a side lobe with an amplitude larger than the main lobe which leads to a false estimate. So examining the value of the cost function only for the possible frequency offsets can help to have a better estimation. Also as there

are fewer pairs to examine for each estimation the computational complexity is a lot fewer.

Although the proposed search algorithm looks at the cost function only at the selected values determined by $\Delta f(m_1, m_2)$ but having local maximums (sidelobes) in the search area in presence of noise limits the estimation range. To avoid this limitation we must increase the distance between these side-lobes and push them out of the search area. This can be done by decreasing the distance between the correlating terms in the cost function. To extend the estimation range we proposed a second preamble structure which is shown in Fig.2(e). This preamble consists of five parts, one cyclic prefix block of length P and two pairs of $(\overline{s}_0, \overline{s}_1)$. Here again \overline{s}_1 is a cyclic shifted version of \overline{s}_0 . Compared to the first proposed preamble the length of the \overline{s}_0 and \overline{s}_1 is reduced to the half and one cyclic prefix block is eliminated. In order to remove the second cyclic prefix the last P samples of the sub-symbols \overline{s}_{00} and \overline{s}_{01} shown in Fig.2(d) should be identical (assuming k < P). This constraint ensures that during the estimation the correlating terms experience same ISI effect.

To estimate the offset, the correlation terms $(a_1$ and $a_2)$ can be calculated separately for each pair of (\bar{s}_0, \bar{s}_1) , and then the corresponding terms summed together to a_1 and a_2 used in (44).

V. SIMULATION RESULTS

For the simulations in this section we consider an OFDM system with 64 sub-carriers, a preamble length of 128 (two blocks) and a channel with L=16 taps and cyclic prefix length P=L and SNR from 6dB to 20dB with AWGN. As mentioned before, both Minn's and Morelli's methods require an FFT operation to determine the frequency offset, and the size of FFT affects the quantization error in the estimation. Our simulation results indicate that in order to have consistent results over the range of SNR, estimation FFT block size (N_{fft}) should at least be 1024. For Minn's method, we assume d=8, and for our first and second proposed methods, we assume k=17 and k=19 respectively. We also consider the cases of d=0 and k=0 to evaluate Morelli's and Schmidl's methods.

Fig. 4 shows the average MSE for the five different methods for different signal to noise ratios when the frequency offset is equal to a sub-carrier bandwidth. It can be observed that all algorithms have very close mean-square error over a wide range of signal to noise ratios.

Table I shows the estimation range for the five methods obtained from simulation. It can be observed that our second proposed method has the largest estimation range. Minn's method can obtain fairly large estimation range at the cost of a large complexity overhead (1024-FFT and multiple correlations). Schmidl's method which is the simplest of all (one correlation calculation) leads to the range of only one sub-carrier spacing. Our first proposed method while having a complexity comparable to Schmidl's method

TABLE I
ESTIMATION RANGE COMPARISON OF DIFFERENT METHODS

Estimation Method	Estimation Range (sub-carrier spacing)
The Second Proposed Method	11.5
Minn	10
The First Proposed Method	5.8
Morelli	5
Schmidl	1

TABLE II
COMPUTATIONAL COMPLEXITY COMPARISON OF DIFFERENT
METHODS

Estimation Method	Computational Complexity (Normalized)
Schmidl	1
The First Proposed Method Independent m_1 and m_2	6.41
The First Proposed Method Related m_1 and m_2	4.37
The Second Proposed Method Independent m_1 and m_2	3.64
The Second Proposed Method Related m_1 and m_2	2.68
Minn	48
Morelli	48

provides a reasonable estimation range, slightly larger than Morelli's method.

Table II³ shows the computational complexity for different preambles. It is obvious that Schmidl's method is the simplest method, so we normalized the computational complexity of all methods to the complexity of this method. Morreli and Minn use an FFT operation to find the correct frequency offset. But this FFT operation adds a high computational complexity to the system. These two methods have a computational complexity 48 times the Schmidl's method. The first proposed method using the first search method (indipendent m_1 and m_2) has a computational complexity only 6.41 times the Schmidl's method. The first proposed method with the second search method which assigns the boundaries of m_2 dynamically has a computational complexity only 4.37 times the Schmidl's method, while having an estimation range 5.8 times the Schmidl's method. The second proposed preamble has the largest estimation range which is 11.5 times Schmidl's method. This preamble using the first search method archives the complexity 3.64 times Schmidl's method and using the dynamic search method with a 30 percent decrease only has a computational complexity 2.68 times Schmidl's method maintaining the 11.5 times Schmidl's method estimation range.

Fig. 5 shows the cost function of the five algorithms in the case where the receiver carrier frequency is equal to the transmitter carrier frequency (zero offset) versus estimated frequency offset (Δf). As can be observed, all the algorithms have a peak at zero (which corresponds to correct estimation). The period of the

³Here we assumed a 1024-point FFT requires 7172 multiplications and 27652 summations, and we further counted every multiplication as 4 additions[19].



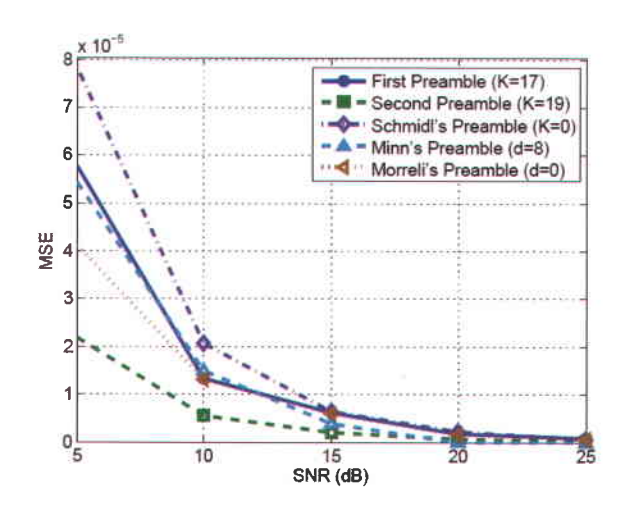


Fig. 4. Average MSE comparison for different frequency offset estimation schemes. k=17 represents the first proposed method, k=19 represents the second proposed method, k=0 represents the Schmidl's method, d=8 represents the Minn's method, d=0 represents the Morelli's method, $\Delta f=0.5\times$ Subcarrier Spacing.

cost function determines the estimation range in high SNR. Estimation range will be limited by minor peaks at low SNR.

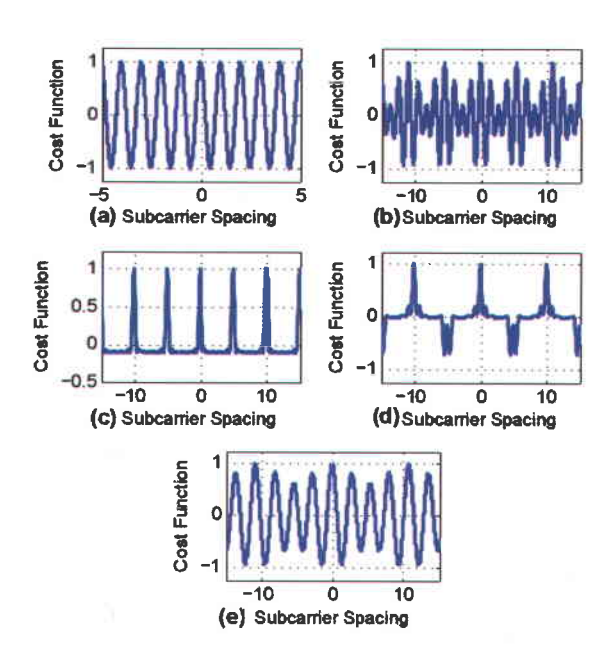


Fig. 5. Cost function versus estimated offset normalized by subcarrier spacing for the case of zero offset between transmitter and receiver (a) Schmidl's Method (b) The First proposed method (c) Morreli's Method (d) Minn's Method. (e) The Second proposed method. (The curves for different frequency offsets are the same except for the shift in the frequency domain.)

VI. CONCLUSION

A unified analysis framework was proposed for ML estimation of carrier frequency offset. We described how different available techniques can be considered as special cases. We further showed through simulations that a 2-symbol preamble structure where the second symbol is a cyclically shifted version of the first symbol can provide a very good compromise

between the extended estimation range and estimation complexity compared to those of other available methods. A second preamble is proposed which has the largest estimation range compared to the reported methods and also its computational complexity is only 2.68 times the simplest method. Furthermore, we proposed a dynamic search method to decrease the computational complexity even more. The Dynamic search method decreases the computational complexity of the proposed methods by about 30 percent.

ACKNOWLEDGMENT

The authors would like to acknowledge support from Iran Telecommunication Research Center (ITRC).

APPENDIX

$\sin \alpha = \alpha$ Justification

Now we justify the approximation used in solving (41) as follows. Let us consider the data model used in section III, $\mathbf{s}_1 = \sqrt{N} \mathrm{diag}\{[\mathbf{F}]_k^H\}\mathbf{s}_0$. As introduced before the transmitted blocks of data after IDFT operation are denoted by $\bar{\mathbf{s}}_0$ and $\bar{\mathbf{s}}_1$. Then,

$$\bar{\mathbf{s}}_{1} = \mathbf{F}^{H} \mathbf{s}_{1}
= \sqrt{N} \left(\mathbf{F}^{H} \operatorname{diag} \{ [\mathbf{F}]_{k}^{H} \} \mathbf{F} \right) \bar{\mathbf{s}}_{0}
= \mathbf{I}_{k} \bar{\mathbf{s}}_{0}$$
(49)

where I_k is the identity matrix circularly right-shifted by k,

$$\mathbf{I}_{k} = \begin{bmatrix} 0 & \dots & 0 & 1 & 0 & \dots & 0 \\ \vdots & \ddots & \vdots & 0 & \ddots & \ddots & \vdots \\ \vdots & \ddots & \vdots & \vdots & \ddots & \ddots & 0 \\ 0 & \dots & 0 & 0 & \dots & 0 & 1 \\ \hline 1 & 0 & \dots & 0 & \dots & \dots & 0 \\ 0 & \ddots & 0 & \vdots & \ddots & \ddots & 0 \\ 0 & \ddots & 1 & 0 & \dots & \dots & 0 \end{bmatrix}$$
(50)

where we used the fact that $\sqrt{N} \mathbf{F}^H \operatorname{diag}\{[\mathbf{F}]_k^H\} \mathbf{F}$ is a circulant matrix whose first row is $\mathbf{F}[\mathbf{F}]_k^H$ which indeed is an all zero vector with a '1' at its $(k+1)_{th}$ position. Therefore, \bar{s}_1 is a circularly shifted version of $\bar{\mathbf{s}}_0$ by k. The corresponding transmitted and received blocks are shown in Fig. 3. Let us assume Δf is a positive offset. Then θ in (8) is basically the phase rotation from one received sample to the next (i.e., $\bar{\mathbf{y}}_0(i)$ to $\bar{\mathbf{y}}_0(i+1)$) due to the frequency offset. Let us consider the first product term in calculating a_1 defined by (39), namely $\bar{\mathbf{y}}_1^H(0)\bar{\mathbf{y}}_0(k)$. Since $\bar{\mathbf{y}}_1^H(0)$ is received after (N+P-k) samples from $\bar{\mathbf{y}}_0(k)$, it is relatively phase rotated by $(N+P-k)\theta$. Therefore the phase of the first product term in a_1 would be -(N + $(P-k)\theta$, if the additive noise would be discarded. Note that the corresponding transmitted samples for these two received samples are identical due to the structure of the transmitted block. Similar argument holds for all the other product terms in calculating a_1 . Therefore, the phase of a_1 will be close to $-(N+P-k)\theta$, given

that the noise contribution is discarded. In other words, the argument $[(N+P-k)\theta+\angle a_1]$ can be considered close to zero. A similar argument holds for the other term, i.e., $[(2N+P-k)\theta+\angle a_2]$ can be considered close to zero.

REFERENCES

- Part 11: Wireless LAN Medium Access Control (MAC) and Physical Layer (PHY) Specifications, Higher-Speed Physical Layer Extension in the 5 GHz Band, IEEE802,11a Jul, 1999.
- [2] IEEE 802.16AB-01/01r1, An air Interface for Fixed Broadband Wireless Access Systems Part A: Systems between 2 and 11 GHz, Jul. 2001.
- [3] Digital Video Broadcasting (DVB-T); Frame Structure, Channel Coding, Modulation for Digital Terrestrial Television, ETS 300 744, Eur. Telecommun. Standard, ETSI. 1997.
- [4] T. Pollet, M. Van Bladel, "BER sensitivity of OFDM to carrier frequency offset and Wiener phase noise," *IEEE Trans. Commun.*, vol. 43, no. 2, Feb. 1995.
- [5] T.Pollet, and M.Moeneclaey, "Synchronizability of OFDM Signals," In Proc. GLOBECOM, Nov. 1995.
- [6] K.Thomas, P.Lorenzo, "Orthogonal frequency division multiplex synchronization techniques for frequency-selective fading channels," *IEEE Journal on Selected Areas in Communications*, Jun. 2001.
- [7] P. H. Moose, "A technique for orthogonal frequency division multiplexing frequency offset correction," *IEEE Transactions on Communications*, vol. 42, pp. 2908-2914, Oct. 1994.
 [8] T. M. Schmidl and D. C. Cox, "Robust frequency and
- [8] T. M. Schmidl and D. C. Cox, "Robust frequency and timing synchronization for OFDM," *IEEE Transactions on Communications*, vol. 45, pp. 1613-1621, Dec. 1997.
- Communications, vol. 45, pp. 1613-1621, Dec. 1997.

 [9] M. Morelli and V. Mengali, "An improved frequency offset estimator for OFDM applications," IEEE Communications Letters, vol. 3, pp. 75-77, Mar. 1999.
- [10] M. Morelli and U. Mengali, "Carrier-Frequency Estimation for Transmissions over Selective Channels," *IEEE Transactions on Communications*, VOL. 48, NO. 9, Sep. 2000.
- [11] H. Minn and P. Tarasak, "Improved Maximum Likelihood Frequency Offset Estimation Based on Likelihood Metric Design," *IEEE Transactions on Signal Processing*, VOL. 54, NO. 6, Jun. 2006.
- [12] Bo Ai and J. Ge, "Frequency Offset Estimation for OFDM in Wireless Communications," *IEEE Trans. on Consumer Electronics*. Feb. 2004.
- [13] K.Thomas and P.Lorenzo, "Orthogonal frequency division multiplex synchronization techniques for frequency-selective fading channels," *IEEE Journal on Selected Areas in Commun.* Jun. 2001.
- [14] K.Bang and N.Cho, "A coarse frequency offset estimation in an OFDM system using the concept of the coherence phase bandwidth," *IEEE Trans. on Commun.* Aug. 2001.
- [15] T. Pollet and M. van Bladel, "BER Sensivity of OFDM systems to carrier frequency offset and Wiener phase noise," *IEEE Trans. Commun.* Feb. 1995.
- [16] X. Ma and H. Kobayashi, "Joint Frequency Offset and Channel Estimation for OFDM," *IEEE Globecom Conf.* Dec. 2003.
- [17] S. Kay, "Fundamentals of Statistical Signal Processing: Estimation Theory," Prentice-Hall, Inc., 1993.
- [18] H. Nezamfar and M.H. Kahaei, "A Comparison Of Maximum Likelihood Frequency Offset Estimation Methods For OFDM Systems," *IEEE* 4th IST 2008 Conf. Aug. 2008.
- [19] http://www.cmlab.csie.ntu.edu.tw/cml/dsp/training/coding/ transform/fft.html



Hooman Nezamfar received the B.Sc. degree in Electrical Engineering from Isfahan University of Technology, Isfahan, Iran in 2004 and the M.Sc. degree in Communication Systems from the Iran University of Science and Technology, Tehran, Iran in 2008. He is currently a Ph.D. student at northeastern university, Boston, USA. During his masters, he worked on the frequency offset estimation in OFDM systems. For his Ph.D. he is interested in

brain computer interfaces.



Mohammad Hossein Kahaei received the B.Sc. degree from Isfahan University of Technology, Isfahan, Iran, in 1986, the M.Sc. degree from the University of the Ryukyus, Okinawa, Japan, in 1994, and the Ph.D. degree in signal processing from the School of Electrical and Electronic Systems Engineering, Queensland University of Technology, Brisbane, Australia, in 1998. He joined the School of Electrical Engineering, Iran University of Science

and Technology, Tehran, Iran, in 1999. His research interests are array signal processing with primary emphasis on adaptive filters theory, blind source separation, localization, tracking, active noise control, and interference cancellation.